Proceedings of the 21st ICSMGE, Vienna, Austria, 14 – 19 June 2026. Pistrol, Adam & Schweiger (eds.)
Published by: ÖGG, Austrian Society for Geomechanics, Salzburg, Austria, ISBN 978-3-9503898-4-5
https://doi.org/10.53243/ICSMGE2026-1857

Real-time Soil Liquefaction Evaluation and Impact Analysis for Earthquake Emergency Management

Bing-Ru Wu, Ming-Wey Huang, and Siao-Syun Ke
National Science and Technology Center for Disaster Reduction, Taiwan, brwu@ncdr.nat.gov.tw

ABSTRACT: Many metropolitan regions in Taiwan are underlain by soft alluvial deposits with high groundwater tables, rendering them highly susceptible to soil liquefaction during strong seismic events. In response to the critical demand for timely and accurate post-earthquake assessments, this study presents the development of an automated, real-time liquefaction analysis module. The system leverages a comprehensive geotechnical database comprising over 40,000 borehole data obtained from both public and private sectors. Distinct from traditional approaches that assume uniform seismic excitation, the proposed framework utilized measured grid-based peak ground acceleration in conjunction with site-specific soil parameters at corresponding grids, thereby enabling reasonable representation of soil behavior in the field. The system automatically generates a suite of disaster response maps, including liquefaction potential and estimated ground settlement distributions in a spatial resolution of 500 m × 500 m, to facilitate rapid evaluation of potential impacts on critical infrastructure. Validation using data from four major earthquake events demonstrates an overall consistency rate of 85% between analytical results and observed liquefaction features. This study offers a robust, real-time decision-support tool that substantially enhances the capabilities in seismic risk mitigation and emergency response planning.

KEYWORDS: soil liquefaction, real-time assessment, emergency management.

1 INTRODUCTION

Taiwan situated along the convergent boundary of the Philippine Sea Plate and Eurasian Plate, renders the island highly vulnerable to seismic hazards. Figure 1 show a dozen of major earthquake records over the past century, notably the Meishan earthquake (M_L = 7.3, 1,258 fatalities) in 1906, Hsinchu-Taichung earthquake (M_L = 7.1, 3,276 fatalities) in 1935, and Chi-Chi earthquake (M_L = 7.3, 2,415 fatalities) in 1999. Approximately 70% of the population resides in six metropolitan regions situated on the western plains, where soft alluvial deposits and high groundwater tables significantly heighten the risk of soil liquefaction during seismic events. Recent earthquakes, such as the Meinong earthquake (M_L= 6.6) in 2016 and the Hualien offshore earthquake (M_L = 7.2) in 2024, further illustrate the remarkable impact of liquefaction-induced ground deformation to buildings and infrastructures. In response to the urgent need for timely disaster impact assessments during emergency operations, this study proposes a real-time liquefaction assessment framework that integrates extensive borehole data with observed ground motion records, thereby improving spatial resolution and enhancing operational applicability.

No.	Earthquake	Date	Magnitude (M_L)	Depth (km)	Casulties	
					Ceased	Injured
1	Douliou	1904/11/06	6.1	7.0	145	158
2	Meishan	1906/03/17	7.1	6.0	1,258	2,385
3	Nantou Series	1916/08/28	6.8	45.0	71	285
		1916/11/15	6.2	3.0		
		1917/01/05	6.2	0.0		
		1917/01/07	5.5	0.0		
4	Hsinchu-TaiChung	1935/04/21	7.1	5.0	3,276	12,053
5	Chungpu	1941/12/17	7.1	12.0	358	766
6	Xinhua	1946/12/05	6.1	5.0	74	182
7	Longitudinal Valley Series	1951/10/22	7.3	4.0	>85	>1,000
		1951/10/22	7.1	1.0		
		1951/10/22	7.1	18.0		
		1951/11/25	6.1	16.0		
		1951/11/25	7.3	36.0		
8	Hengchun	1959/08/15	7.1	20.0	17	85
9	Paiho	1964/01/18	6.3	18.0	106	653
10	Hualien	1986/11/15	6.5	15.0	13	45
11	Chi-Chi	1999/09/21	7.3	8.0	2,415	11,305
12	Jiaxian	2010/03/04	6.4	5.0	0	96
13	Meinong	2016/02/06	6.6	14.6	117	504
14	Hualien	2018/02/26	6.2	6.3	17	291
15	Chishang	2022/9/18	6.8	7.8	1	97
16	Hualien offshore	2024/04/03	7.2	15.5	17	1,155

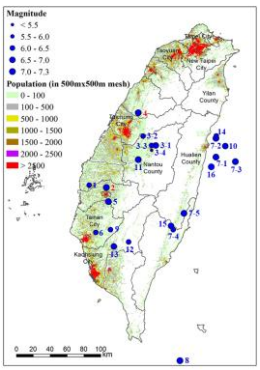

Figure 1. Location of disastrous earthquakes and population distribution in Taiwan

2 LIQUEFACTION ANALYSIS METHODOLOGY

2.1 *Overview of relative researches*

To identify areas susceptible to soil liquefaction, the International Society for Soil Mechanics and Geotechnical Engineering (ISSMGE, 1999) proposed a hierarchical zonation framework comprising three levels of analysis, each tailored to a specific mapping scale and data availability. Grade 1 zoning is suited for regional-scale assessments at mapping scales between 1:1,000,000 and 1:50,000. It utilizes geological and geomorphological maps, historical earthquake records, and other existing datasets. Grade 2, appropriate for intermediate scales ranging from 1:100,000 to 1:10,000, incorporates aerial photography, remote sensing data, field reconnaissance, and community interviews to refine susceptibility delineation. Grade 3 involves site-specific investigations, relying on detailed geotechnical exploration and analysis, and is applied at finer scales between 1:25,000 and 1:5,000.

The Federal Emergency Management Agency (FEMA, 2013) developed a methodology under the HAZUS multi-hazard loss estimation platform to assess liquefaction susceptibility. This approach assigns qualitative susceptibility ratings—ranging from very low to very high—based on factors such as geologic age, depositional environment, and the spatial distribution of cohesionless sediments. The rating scheme builds upon the classification system introduced by Youd and Perkins (1978), which is particularly effective for regional-scale mapping. The U.S. Geological Survey has applied this methodology to generate susceptibility maps for regions such as the San Francisco Bay Area.

For local-scale assessments, a variety of simplified procedures have been developed to evaluate liquefaction potential using site-specific data. These methods typically incorporate blow counts from the standard penetration test (SPT-N value), peak ground acceleration (PGA), earthquake magnitude, groundwater table depth, and subsurface soil properties obtained through borehole investigations (Seed and Idriss, 1971; Seed et al., 1985; Tokimatsu and Yoshimi, 1983; Japan Road Association, 1996). Furthermore, probabilistic frameworks have also been proposed to estimate the likelihood of liquefaction occurrence, offering a quantitative alternative to deterministic approaches (Liao et al., 1988; Juang et al., 1999, 2000; Huang et al., 2004).

After the 1999 Chi-Chi earthquake, a national research program funded by the National Science and Technology Council (Lin et al., 2001) compiled engineering borehole data to produce preliminary liquefaction potential maps for ten cities and counties across Taiwan using three simplified evaluation techniques. Subsequently, following the 2016 Meinong

earthquake, the Geology Survey and Mining Management Agency (GSMMA) published intermediate-scale liquefaction potential maps for all 22 cities and counties in Taiwan to support disaster risk reduction and planning initiatives.

Despite these efforts, most liquefaction potential maps are based on deterministic seismic scenarios, applying a fixed earthquake magnitude and a uniform design-level PGA as specified by building codes. Such assumptions may not accurately capture the variability in ground motion characteristics during actual seismic events and, consequently, may fail to reflect the spatial variability in liquefaction responses. Furthermore, there remains no available methodology for real-time mapping of liquefaction following a major earthquake. This underscores the need for a rapid assessment approach that integrates earthquake magnitude and spatially distributed, real-time PGA measurements to facilitate informed decision-making during emergency response operations.

2.2 *Integration of borehole database*

To facilitate a more refined assessment of liquefaction potential in urban environments, multiple engineering borehole databases have been established by government agencies and research institutions in Taiwan. Following the 1999 Chi-Chi earthquake, approximately 8,700 borehole records were collected through the National Liquefaction Potential Map Project (Lin et al., 2001) in collaboration with academic institutions. In addition, 73 new boreholes were drilled at sites exhibiting both liquefaction and non-liquefaction behavior.

In 2010, the GSMMA compiled the Engineering Geological Borehole Database, aggregating borehole data primarily derived from infrastructure construction projects, including highways, mass transit systems, and municipal utilities such as water supply and sewerage networks. As illustrated in Figure 2, the 2015 version of this database included more than 15,000 boreholes. However, the spatial distribution of these data points is largely linear, mirroring the alignments of infrastructure corridors. This distribution pattern results in limited coverage of alluvial plains and constrains the utility of the dataset for comprehensive liquefaction hazard evaluations.

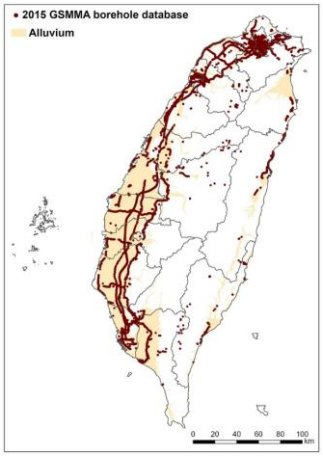

Figure 2. The engineering borehole database established by GSMMA in 2015

To address these limitations and improve spatial representativeness, additional borehole data were collected from a broad array of public and private sector sources. These included contributions from GSMMA, the Central Weather Administration (CWA), the Yilan County Government, engineering consultant company, and post-earthquake investigations conducted by the National Center for Research on Earthquake Engineering (NCREE) at documented Chi-Chi earthquake liquefaction sites. The integrated dataset compiled in this study comprises over 40,000 borehole records (Figure 3), representing a 2.5-fold increase relative to the 2015 GSMMA database. This updated 2025 version provides substantially improved coverage of alluvial deposits and establishes a more robust foundation for accurate and reliable liquefaction potential assessments.

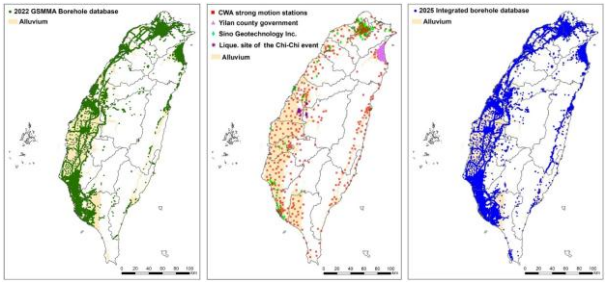

(a) GSMMA borehole database in 2022 (b) Borehole data from public and private sectors (c) Integrated borehole database

Figure 3. The borehole database compiled in this study

2.3 *Real-time liquefaction analysis module*

The real-time liquefaction analysis module was established in this study using the evaluation procedure proposed by the Japan Road Association (1996), which was recommended in the current seismic design code for buildings in Taiwan (National Land Management Agency, 2022). The method incorporates various geotechnical parameters obtained from borehole investigations, including Standard Penetration Test (SPT) N-values, fines content (FC), grain size distribution parameters (D_{50}, D_{10}), plasticity index, groundwater table depth, and effective overburden pressure (σ_v'), to calculate the cyclic shear strength ratio (R).

The cyclic shear stress ratio (L) for the soil strata is determined based on the Peak Ground Acceleration (PGA), the depth-dependent shear stress reduction coefficient (r_d), total overburden pressure (σ_v), and effective overburden pressure (σ_v'). The safety factor against liquefaction (F_L) is defined as the ratio of the cyclic shear strength ratio (R) to the cyclic shear stress ratio (L). A safety factor less than 1.0 indicates a high likelihood of initial liquefaction occurring under the specified seismic loading conditions.

Considering the influence of overburden pressure, liquefaction occurring at greater depths typically exerts less impact on structures and critical infrastructure near the surface. To address this effect, Iwasaki et al. (1982) introduced the Liquefaction Potential Index (P_L), which evaluates the liquefaction potential of soil layers to a depth of 20 meters, incorporating a depth-dependent weighting factor, $w(z)$, to reflect the reduced surface impact of liquefaction at greater depths.

$$P_L = \int_0^{20} F(z) \times w(z) dz \tag{1}$$

where z is the depth (m)

$w(z)$=10-0.5z

when $F_L \leqq 1.0$, $F(z)$=1- F_L

$F_L > 1.0$, $F(z)$=0.

Based on field observations from several earthquake events, soil liquefaction potential, as indicated by P_L, can be categorized into three levels:

1. Low potential: $0 < P_L \leqq 5$, low likelihood of liquefaction occurrence;

2. Moderate potential: $5<P_L \leqq 15$, liquefaction may occur in deeper soil layers, with some surface manifestations potentially observable;
3. High potential: $P_L > 15$, high likelihood of liquefaction, with distinct surface features such as sand boils, ground settlement, or lateral spreading commonly observed.

Once a significant earthquake occurred, the Central Emergency Operation Center (CEOC) is promptly activated to facilitate emergency response efforts among government agencies. To deliver the decision supporting information to the commander of the CEOC, an automated module for soil liquefaction analysis has been developed to provide real-time evaluation of soil liquefaction and induced ground settlements (Figure 4).

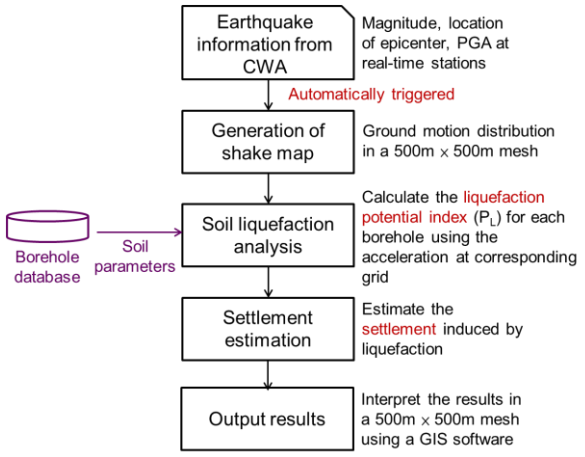

Figure 4. Automated processing module for soil liquefaction analysis

1. Activation of the processing module: Upon receipt of an earthquake report from the CWA via email, the soil liquefaction analysis module is automatically triggered. Key seismic parameters, including earthquake magnitude, epicenter location, and PGA recorded at real-time monitoring stations, are extracted from the report.
2. Generation of Shake Map: A shake map is generated using the recorded PGA values to represent the spatial distribution of ground shaking intensity. The ground motion is interpolated onto a 500 m × 500 m grid, which serves as the input motion for subsequent soil liquefaction analysis.
3. Soil Liquefaction Analysis: The Liquefaction Potential Index (P_L) is calculated for each borehole location using geotechnical parameters retrieved from the borehole database based on Equation 1. Utilizing the grid-based PGA distribution in conjunction with soil parameters at corresponding grid enables a more realistic estimation of the soil response.
4. Settlement Estimation: Liquefaction-induced settlement within each soil layer is estimated based on the empirical correlation between the factor of safety against liquefaction (F_L) and post-liquefaction volumetric strain (ε_v) proposed by Ishihara and Yoshimine (1992). The total ground settlement is computed as the sum of the volumetric strains across all liquefied soil layers.

$$S = \sum_{i=1}^{NL} \varepsilon_{v,i} \Delta H_i \qquad (2)$$

5. Output of Results: The soil liquefaction hazard map is automatically generated on a 500 m × 500 m grid. The estimated liquefaction-induced settlement is further utilized to assess potential impact to critical infrastructure, including bridges and underground pipelines.

3 PERFORMANCE VALIDATION USING FIELD OBSERVATIONS FROM FOUR EARTHQUAKE EVENTS

To assess the performance of the proposed methodology, four significant earthquake events from the past 25 years were selected for soil liquefaction analysis, including the 0921 Chi-Chi earthquake in 1999, 0206 Meinong earthquake in 2016, the 0206 Hualien earthquake in 2018, and 0403 Hualien earthquake in 2024. Liquefaction records from these reconnaissance reports were retrieved to compare with the analytical results.

As defined in Equation (1), the P_L value greater than 5 indicates a likelihood of observable surface manifestations of liquefaction. For validation purposes, the results were considered consistent if field evidence of liquefaction was observed at locations with $P_L > 5$, or if no liquefaction features were detected at sites with $P_L \leq 5$. Cases where $P_L > 5$ but no liquefaction was observed in the field were classified as overestimated. Conversely, instances in which liquefaction features were documented at sites with $P_L \leq 5$ were categorized as underestimated. Table 1 provides the basic information for each earthquake event, the number of liquefaction records, and a comparison of results based on a total of 713 liquefaction observations.

Table 1. Comparison of analytical results with liquefaction records for 4 earthquake events.

Date	Event	Mag-nitude (M_L)	No. of records	Consistent with field observation	Over-estimated	Under-estimated
1999/9/21	Chi-Chi earthquake	7.3	189	159	21	9
2016/2/6	Meinong earthquake	6.6	496	423	0	73
2018/2/6	Hualien earthquake	6.2	23	19	0	4
2024/4/3	Hualien earthquake	7.2	5	5	0	0
Total			713	606	21	86

3.1 *0921 Chi-Chi earthquake in 1999*

On September 21, 1999, a catastrophic earthquake with a local magnitude (M_L) of 7.3 struck central Taiwan, resulting in over 2,400 fatalities, more than 10,000 injuries, and the destruction or significant damage of approximately 100,000 buildings. Critical infrastructure, including roads, bridges, potable water systems, and power supplies, sustained extensive damage, with some regions remaining inaccessible for several days. Widespread soil liquefaction occurred in alluvial deposits across Taichung City, Nantou County, and Changhua County, leading to considerable settlement and tilting of buildings, failure of quay walls in ports, and lateral spreading along riverbanks. These phenomena severely compromised the structural integrity and operational functionality of both buildings and essential lifeline systems.

Using PGA data recorded by strong-motion stations from the CWA, a shake map of the Chi-Chi earthquake was generated on a 500 m × 500 m grid (Figure 5). Areas exhibiting PGA values exceeding 400 gal encompassed six cities and counties in central Taiwan. By integrating the earthquake magnitude, the spatial distribution of PGA, and soil properties derived from borehole data at corresponding grid points, the liquefaction potential was assessed, as shown in Figure 6.

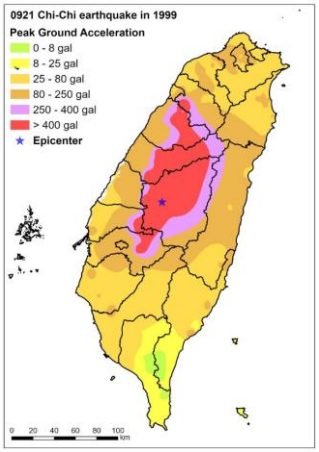

Figure 5. Measured peak ground acceleration for the 0921 Chi-Chi earthquake in 1999

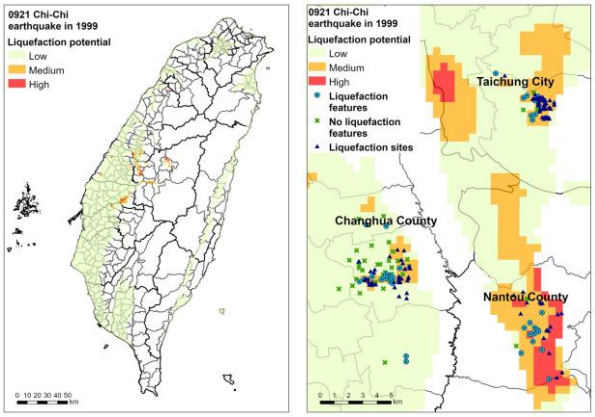

Figure 6. Comparison of analytical results and field observations for the Chi-Chi earthquake

Among the 73 boreholes drilled at liquefied and non-liquefied sites, 30, which exhibited liquefaction features, were located within grid cells where P_L value exceeded 5, while 26 boreholes, devoid of liquefaction evidence, were situated in areas with $P_L \leq 5$. Additionally, of the 116 liquefaction sites identified by Lin et al. (2001), 103 were found within grid cells where $P_L > 5$.

In total, 159 out of 189 data points (84%) showed consistency between the analytical predictions and field observations. The analysis also revealed 21 instances (11%) of over-estimation, where $P_L > 5$ but no liquefaction was observed, and 9 instances (5%) of under-estimation, where liquefaction features were present in regions with $P_L \leq 5$. These findings underscore high reliability of the proposed method for assessing liquefaction potential during the Chi-Chi earthquake.

3.2 *0206 Meinong earthquake in 2016*

A magnitude (M_L) 6.6 earthquake occurred on February 6, 2016 in the Meinong District of Kaohsiung City, resulting in 117 fatalities, over 500 injuries, the collapse of one building, and extensive structural damage to numerous others. The distribution of recorded ground motion (Figure 8) shows the PGA values in the most affected areas ranged from 250 to 400 gal.

Although the earthquake epicenter was located in the Meinong District of Kaohsiung City, the most significant liquefaction effects were observed in the Annan, Xinhua, and Xinshi Districts of Tainan City. These impacts were largely attributed to the unfavorable local soil conditions and shallow groundwater levels. Notably, Annan District sustained the most extensive liquefaction damage, as it is underlain by coastal alluvial deposits and former lagoon sediments composed primarily of loose, saturated sands and silts—materials that are particularly susceptible to liquefaction under seismic loading.

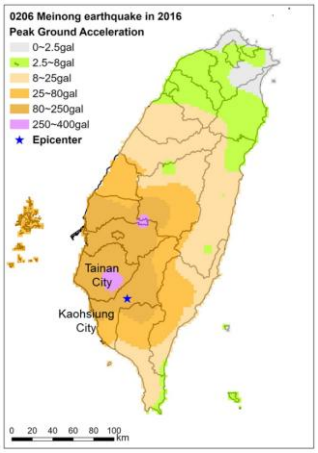

Figure 7. Measured peak ground acceleration for the 0206 Meinong earthquake in 2016

The quantity and spatial distribution of borehole data, particularly in regions underlain by alluvial deposits, are critical determinants of the reliability of soil liquefaction analysis. In this study, borehole data compiled over the past 25 years from both public and private sources were integrated to enhance the analytical framework. As shown in Figure 8(a), the 2015 GSMMA borehole database for Tainan City exhibits a predominantly linear distribution, which fails to uniformly cover the alluvial deposits. In contrast, the 2025 integrated borehole database, presented in Figure 8(b), demonstrates a significant improvement in spatial coverage across the target areas.

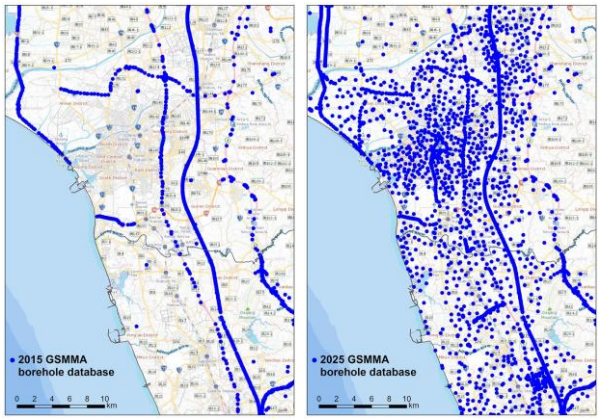

(a) 2015 GSMMA borehole database (b) 2025 Integrated borehole database

Figure 8. Distribution of borehole databases established in 2015 and 2025 for Tainan City

When the 2016 Meinong earthquake occurred, the automated soil liquefaction analysis module was activated to generate liquefaction potential maps (Figure 9) using the 2015 GSMMA borehole data. These maps were incorporated into the decision-support information provided to the CEOC during the emergency response. The analysis revealed extensive areas of moderate to high liquefaction potential in the Annan District. The evaluation results were generally consistent with the liquefaction effects observed in both the Annan and Xinshi Districts. However, in the Xinhua District, the limited availability of borehole data diminished the reliability of the assessment, leading to a lower level of confidence in the predicted liquefaction potential for this area.

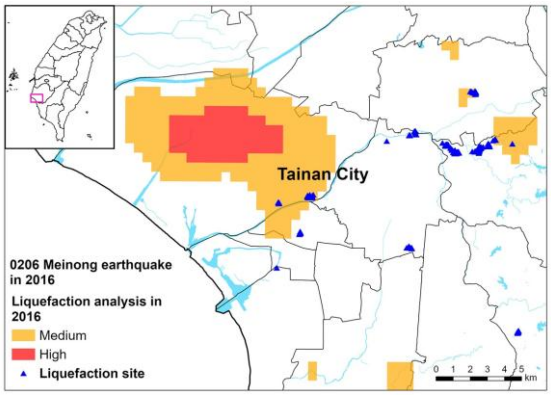

Figure 9. Comparison of liquefaction analysis in 2016 using 2015 GSMMA borehole database and field observations

Using the 2025 integrated borehole database, the liquefaction potential was re-assessed for regions previously lacking sufficient borehole data (Figure 10). Compared to the earlier results presented in Figure 9, the extent of high liquefaction potential zones in the Annan District was reduced, leading to a more accurate representation of soil responses in the field. Notably, clusters of sand boils observed in the alluvial regions between two streams in Xinhua District have been repeatedly present in the 1946 Xinhua earthquake (M_L = 6.1), the 2010 Jiaxian earthquake (M_L = 6.4) and this event. The updated assessment more effectively captures the liquefaction potential of these historically affected areas.

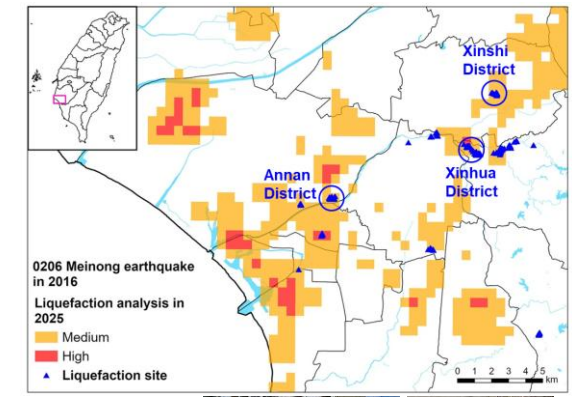

(a)Settlement in Annan District (b)Settlement in Xinshi District (c)Sand boil in Xinhua District

Figure 10. Comparison of liquefaction analysis using 2025 integrated borehole database and field observations

A total of 496 liquefaction records were compiled from post-event investigations conducted by the GSMMA (2016), the National Science and Technology Center for Disaster Reduction, and the National Center for Research on Earthquake Engineering (NCDR and NCREE, 2016). Of these, 423 records (85%) were consistent with the analytical results, while 73 records (15%) showed under-estimation. Overall, the evaluation demonstrates acceptable performance in assessing liquefaction potential during the 2016 Meinong earthquake.

3.3 *Two earthquakes in Hualien County*

Two major earthquakes took place in the Hualien offshore regions: the 0206 Hualien earthquake (M_L = 6.2) in 2018 and the 0403 Hualien earthquake (M_L = 7.2) in 2024. Figure 11 illustrates the intensity distributions for both events. Because of larger magnitude, the 2024 earthquake caused more severe destruction to buildings in wider region and widespread landslides in Taroko National Park. In contrast, the 2018 earthquake induced more localized impact, with damage primarily attributed to structural vulnerabilities in buildings. Both events resulted in recurrent instances of soil liquefaction in areas known to be geologically susceptible. These repeated occurrences underscore the critical importance of identifying and mitigating liquefaction risks in such vulnerable regions.

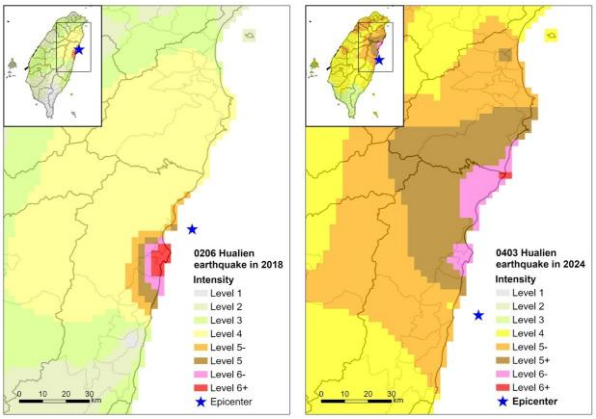

(a) 0206 Hualien earthquake in 2018 (b) 0403 Hualien earthquake in 2024

Figure 11. Intensity maps for two earthquakes in Hualien County

For the 2018 event, typical soil liquefaction manifestations, including sand boils, lateral spreading, and ground settlement, were observed along Huaxi Road (a former wetland area), the riverbanks of the Meilun Stream, and within the Hualien Port region (GSMMA, 2018; NCREE, 2018). As illustrated in Figure 12, the analytical results identified medium liquefaction potential zones that encompassed 19 out of the 23 reported liquefaction sites, yielding a consistency rate of 82.6%.

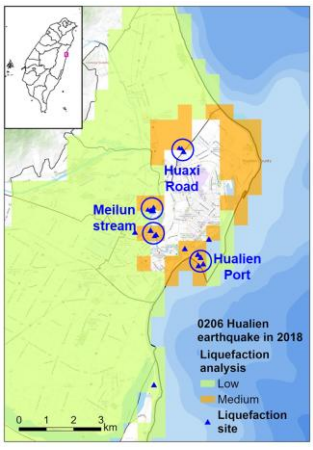

(a)Settlement and Lateral spreading along Meilun stream

(b)Sand boil by Huaxi Road

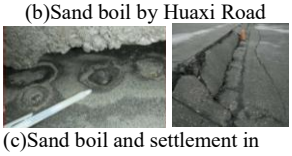

(c)Sand boil and settlement in Hualien Port

Figure 12. Comparison of liquefaction analysis and field observations for the 0206 Hualien earthquake in 2018

According to the reconnaissance report for the 2024 event (NCREE, 2024), liquefaction features were again observed along the riverbanks of the Meilun Stream and in the Hualien Port region. All liquefaction sites were located in areas with medium liquefaction potential identified by the analytical results (Figure 13).

In summary, the proposed assessment approach demonstrated an overall consistency rate of 85% when compared with 713 documented liquefaction records from four major earthquake events, highlighting its effectiveness and reliability for post-earthquake liquefaction evaluation.

4 LIQUEFACTION IMPACT THEME MAP

During seismic events, the ground settlement, lateral spreading, and differential displacement induced by soil liquefaction could compromise the structural integrity and operational functionality of critical infrastructure such as airports, port facilities, and river embankments. Based on liquefaction analytical results, a liquefaction impact theme map can be produced to identify high-risk zones and highlight the potential effects on critical infrastructure. Figure 13 was the liquefaction impact theme map generated during emergency response for the 0206 Hualien earthquake in 2018.

Liquefaction at airports can damage runways, utility systems, and disrupting air traffic during emergency response. In ports, it may cause quay wall failure, and crane collapse, impacting marine transport and cargo operation. Liquefied river embankments can lead to slope instability or failure, heightening flood risks. These recurring issues emphasize the need for thorough liquefaction hazard assessments and mitigation strategies for critical infrastructure. The thematic map provides valuable reference for authorities of critical facilities to take corresponding actions and formulate appropriate disaster prevention measure to reduce the seismic impact.

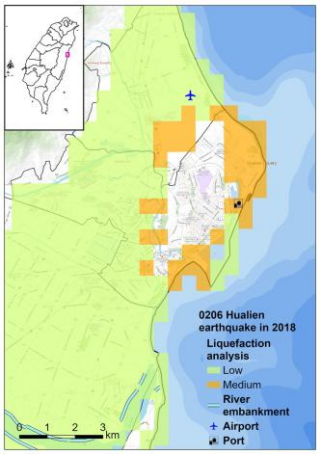

Figure 13. Liquefaction impact theme map for the 0206 Hualien earthquake in 2018

5 CONCLUSIONS

1. Enhanced Liquefaction Hazard Mapping: The integration of real-time seismic data with extensive borehole records significantly improves the spatial resolution and accuracy of liquefaction hazard assessments. This enables more reliable identification of high-risk zones in urban areas, ensuring targeted mitigation efforts for infrastructure protection during seismic events.
2. Real-Time Disaster Response Support: The developed real-time liquefaction analysis module enhances emergency response capabilities by automatically generating liquefaction impact maps during seismic events. This provides critical decision-making support for disaster management agencies, allowing them to quickly assess liquefaction risks to critical infrastructure and prioritize mitigation measures.
3. Validation and Performance: The proposed methodology, validated through four major earthquake events, demonstrated a high level of consistency with field observations (85% accuracy). This confirms the reliability of the approach for post-earthquake liquefaction evaluation, underscoring its effectiveness for enhancing disaster preparedness and resilience in seismic-prone regions.

6 ACKNOWLEDGEMENTS

The authors would like to acknowledge the grant support from the National Science and Technology Council (NSTC 113-2124-M-865-001). The borehole databases provided by the GSMMA, CWA, NCREE, and Sino Geotechnology Inc. are greatly appreciated.

7 REFERENCES

Geology Survey and Mining Management Agency, 2016. *Geological survey report for the 20160206 earthquake*, Ministry of Economic Affairs, Taiwan, ROC. (in Chinese).

Geology Survey and Mining Management Agency, 2018. *Preliminary geological survey report for the 0206 Hualien earthquake in 2018*, Ministry of Economic Affairs, Taiwan, ROC. (in Chinese).

Hwang, J. H., Yang, C. W., and Juang, D. S. 2004. A practical reliability-based method for assessing soil liquefaction potential, *Soil Dynamics and Earthquake Engineering*, 24, 761-770

International Society for Soil Mechanics and Geotechnical Engineering, 1999. *Manual for zonation on seismic geotechnical hazards (revised version)*, Technical Committee for Earthquake Geotechnical Engineering, TC4.

Ishihara K., and Yoshimine, M. 1992. Evaluation of settlements in sand deposits following liquefaction during earthquake, *Soils and Foundations*, 32(1), 173-188.

Iwasaki T., Arakawa, T., and Tokida, K. 1982. Simplified procedures for assessing soil liquefaction during earthquake, *Proc., the Conference on Soil Dynamics and Earthquake Engineering*, Southampton, 925-939.

Japan Road Association, 1996. *Road Bridge Specifications: Part V Series of Earthquake Seismic Design*, Tokyo. (in Japanese).

Juang, C. H., Chen, C. Jiang, J., T., and Andrus, R. D. 2000. Risk-based liquefaction potential evaluation using standard penetration tests, *Canadian Geotechnical Journal*, 37, 1195-1208.

Juang, C. H., Rosowsky, D., and Tang, W. H. 1999. Reliability-based method for assessing liquefaction potential of soils, *J. of Geotechnical and Geoenvironmental Engineering, ASCE*, 125(8), 684-689.

Ke, Y. Y. 2018. Field observation of liquefaction and induced settlement for the Hualien earthquake, Department of Civil Engineering, National Cheng Kung University, Taiwan, ROC (in Chinese).

Liao, S. S., Veneziano, C., D., and Whitman, R. V. 1988. Regression models for evaluation liquefaction probability, *J. of Geotechnical Engineering, ASCE*, 114(4), 389-409.

Lin, M. L., Chen, M. H., and Shen, C. C. 2001. *Production of national liquefaction potential maps and research on evaluation methods*. National Center for Research on Earthquake Engineering, Taiwan, ROC (in Chinese).

National Center for Research on Earthquake Engineering, 2018. *Reconnaissance report of seismic damages caused by the 6 February 2018 Earthquake, Hualien, Taiwan* (in Chinese).

National Center for Research on Earthquake Engineering, 2024. *Summary report for the 2024-04-03 Hualien earthquake, Taiwan, ROC* (in Chinese).

National Science and Technology Center for Disaster Reduction and National Center for Research on Earthquake Engineering, 2016. *Summary report for the 0206 earthquake disaster information and field investigation, Taiwan, ROC* (in Chinese).

National Land Management Agency (2022). *Seismic design code for buildings* (in Chinese), Taiwan, ROC.

Seed, H. B., and Idriss, I. M. 1971. Simplified procedure for evaluating soil liquefaction potential, *J. of the Soil Mechanics and Foundations Division, ASCE*, 97(9), 1249-1273.

Seed, H. B., Tokimatsu, K., and Harder, L. F. 1985. Influence of SPT procedure in soil liquefaction resistance evaluations, *J. of Geotechnical Engineering, ASCE*, 111(12), 1425-1445.

Tokimatsu, K., and Yoshimi, Y. 1983. Empirical correlation of soil liquefaction based on SPT N-value and fines content, *Soils and Foundations*, 23(4), 56-74.

Youd, T. L., and Perkins, D. M. 1978. Mapping liquefaction-induced ground failure potential, *J. of Geotechnical Engineering, ASCE*, 104, no. 4, 433–446.